Journal Pre-proof

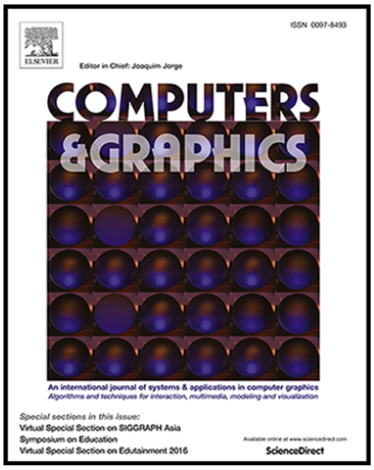

Physicalizing cardiac blood flow data via 3D printing

Kathleen D. Ang, Faramarz F. Samavati, Samin Sabokrohiyeh, Julio Garcia, Mohammed S. Elbaz

PII: S0097-8493(19)30155-4
DOI: https://doi.org/10.1016/j.cag.2019.09.004
Reference: CAG 3132

To appear in: *Computers & Graphics*

Received date: 18 March 2019
Revised date: 12 July 2019
Accepted date: 18 September 2019

Please cite this article as: Kathleen D. Ang, Faramarz F. Samavati, Samin Sabokrohiyeh, Julio Garcia, Mohammed S. Elbaz, Physicalizing cardiac blood flow data via 3D printing, *Computers & Graphics* (2019), doi: https://doi.org/10.1016/j.cag.2019.09.004

Highlights

- Blood flow data from 4D Flow MRI can be visualized using affordable 3D printers
- Flow physicalization is a tangible alternative to digital 3D flow visualizations
- The presented physicalization framework can be applied to real medical data

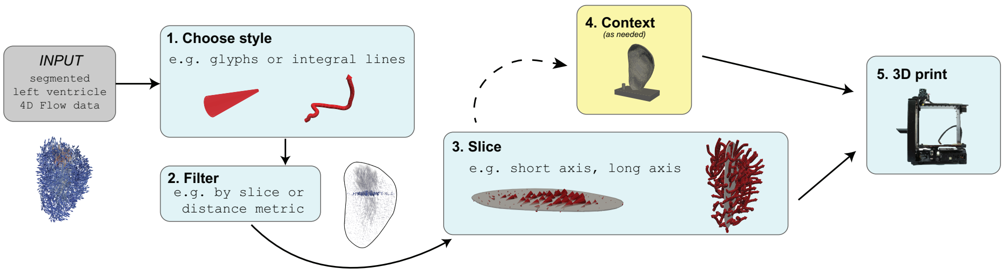
INPUT
segmented
left ventricle
4D Flow data
1. Choose style
e.g. glyphs or integral lines
2. Filter
e.g. by slice or
distance metric
3. Slice
e.g. short axis, long axis
4. Context
(as needed)
5. 3D print

Computers & Graphics (2019)

Contents lists available at ScienceDirect

Computers & Graphics

journal homepage: www.elsevier.com/locate/cag

Physicalizing cardiac blood flow data via 3D printing

Kathleen D. Ang[a,*], Faramarz F. Samavati[a], Samin Sabokrohiyeh[a], Julio Garcia[a], Mohammed S. Elbaz[a]

[a] *University of Calgary, Calgary, Canada*

ARTICLE INFO

Article history:
Received September 27, 2019

Keywords: Physical visualization, 3D printing, 4D Flow MRI, Biomedical applications

ABSTRACT

Blood flow data from cardiac 4D Flow MRI (magnetic resonance imaging) holds much potential for research and diagnosis of flow-related diseases. However, understanding this data is quite challenging – after all, it is a volumetric vector field that changes over time. One helpful way to explore the data is by flow visualization, but most traditional flow visualizations are designed for 2D screens and thus suffer from limited depth perception and restricted screen space. We propose a novel slice-based physical model as a complementary method for visualizing the flow data. The design of this model respects the conventional method of viewing medical imagery (i.e. in cross sections) but has the added advantages of engaging one's sense of touch, not suffering from screen space restrictions, and being easily fabricated by affordable fused deposition modeling (FDM) printers. We apply the slice-based technique to different representations of blood flow data and demonstrate that the technique is capable of transforming volumetric flow data into a tangible, easily fabricable model.

1. Introduction

Medical imaging illuminates the unseen in modern-day medicine; it empowers our ability to understand the human body in both its beauty and its struggles, with usage in areas such as research, diagnosis, and communication. In recent years, imaging technology has reached a point where even blood flow in the heart and great vessels can be acquired. One such technology, known as 4D Flow MRI (magnetic resonance imaging), captures time-varying three-dimensional data that represents the magnitude and direction of blood flow [1]. While 4D Flow MRI holds much potential for research and diagnostic tests of flow-related diseases [2], to understand this data we need a way to visualize it.

Due to the complexity of the data – it is volumetric, time varying, and encodes vector field information – creating good visualizations can be quite challenging. Common ways for visualizing vector field data include using *glyphs* as a visual representation of the vectors at each point in space, or using *integral lines* such as streamlines or pathlines, which are tangent to the vector field at every point and can depict complex flow patterns [1]. Some medical imaging software programs are also equipped with tools for volume rendering, accompanied by interaction techniques such as rotating, zooming in/out, and panning. Although such programs are beneficial, there are some drawbacks: it can take some time to learn how to use the software (even interaction with mouse/keyboard can limit accessibility to a broader audience), and the visualizations are ultimately displayed on a 2D screen. Thus, challenges with screen space, depth perception, lack of tangibility, and understanding of real-world physical scale are inevitable.

Rather than navigating the constraints that are imposed by 2D screen visualizations, we propose the use of *physical visualization* or *physicalization* (we use these terms interchangeably) as a technique to represent blood flow data. A fabricated model offers natural depth perception (since it inherently exists in 3D space) as well as the advantage of tangibility. There are a number of reported benefits of physical visualization, such as enabling active perception, appealing to non-visual senses,

*Corresponding author:
e-mail: kdang@ucalgary.ca (Kathleen D. Ang)

making data more accessible to a broader audience (e.g. those who are visually impaired or who are less amenable to digital technology), and engaging people [3]. In medicine specifically, there has been a marked increase in the use of physical models (i.e. 3D printed models) over the last two decades [4, 5, 6, 7]. Various types and applications of models exist, ranging from customized 3D-printed implants [8] to prints of patient-specific anatomy for presurgical planning [9]. Given that synthesis of data from different sources (e.g. anatomical structures from cine SSFP (steady-state free precession) MRI and blood flow from 4D Flow MRI) is often desirable for increased understanding and analysis, physicalization of blood flow holds promise for enhancing the more typical anatomical 3D printed models in medicine. But despite the growing body of work focused on 3D printing in medical applications, to the authors' best knowledge there have been no studies on 3D printing for visualization of blood flow data.

Indeed, physically visualizing volumetric vector field data is challenging. Fundamentally, it requires designing a model that can be fabricated by tangible material, which can take place in many ways (e.g. subtractive manufacturing, additive manufacturing, or careful design and assembly at the hand of an artist, to name a few). To encourage accessibility to a wider audience, we chose to use affordable material extrusion 3D printers (often referred to as "fused deposition modelling (FDM)" or "fused filament fabrication (FFF)" printers). From here, we must consider *how* vector field data can be visualized. Typical flow visualization styles such as vector glyphs or streamlines are common for digital fomats, but it is not straightforward to fabricate a comparable physical visualization with potentially many glyphs, or long and thin streamlines, since such fine features are susceptible to breakage [10]. Moreover, there are other subtleties to consider when creating a physical visualization – unlike virtual visualizations, physical models are subject to gravity and need appropriate mechanisms for existing in the real world [3]. Hence, naïvely attempting to print some glyphs or streamlines is essentially guaranteed to fail (Fig. 1).

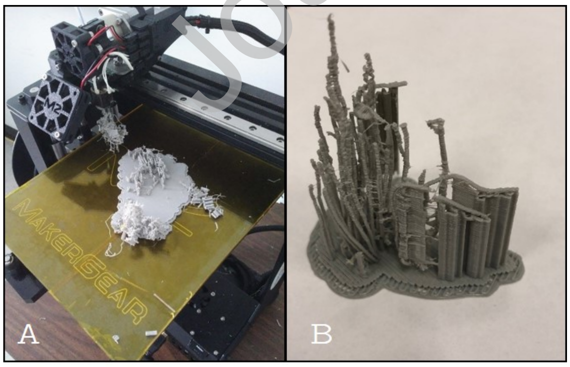

Fig. 1. Some initial tests: (A) Attempting to print a small sample of thin arrow glyphs failed due to the many fragile features; and (B) Trying to print a small sample of streamlines shows that thin tubes are quite breakable.

To tackle these challenges, our physical visualization design was inspired by traditional methods that are natural to most medical professionals: slice-based (i.e. cross section-based) visualization. Typical practice in the medical community involves viewing "slices" or cross sections (2D images) of the data, as this better supports detailed analysis [11] and is the format of most medical images, even if a volumetric space was acquired. Specifically, our slice-based physical visualization is constructed in 5 main steps (see also Fig. 2):

1. Select a visualization style to represent the data. We primarily focus on two styles, glyphs and integral lines.
2. Filter the visualization objects (i.e. glyphs or lines) so that they are fabricable, either by subsampling (for the glyphs), or by using a *similarity-guided* placement strategy [12] (for the streamlines).
3. "Slice" the model into 3D printable parts which are subsets of the original dataset.
4. Augment the model with anatomical context and auxiliary structures (e.g. base/connecting parts) as appropriate.
5. Fabricate the model using an affordable 3D printer.

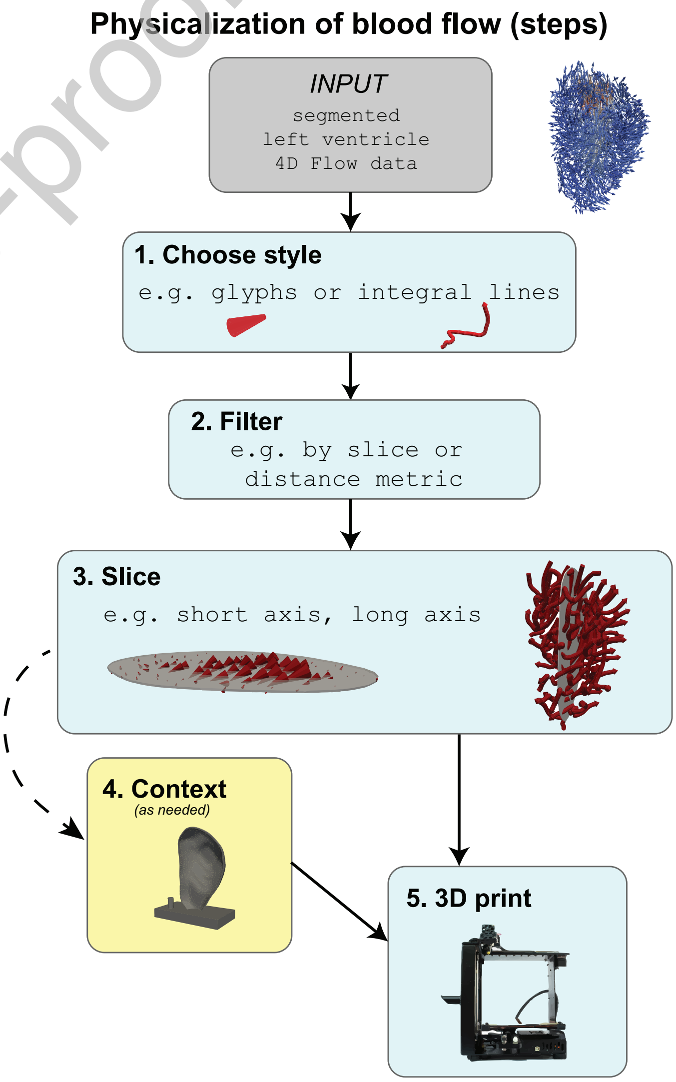

Fig. 2. Overview of physical visualization framework.

The slice-based design brings with it numerous advantages: it creates an inherent support structure which can be easily fabricated by low-cost 3D printers, it affords a potential way to compare between different parts of the data (e.g. comparing slices from two different time frames), and it naturally adds contextual information. The palpability of the overall model can also be seen as a complementary means to grasp the data. Moreover, our physical flow model can be used to enhance anatomical 3D printed models by providing complementary hemodynamic information.

The main contributions of this work include the following:

1. Developing a new framework for physical visualization of cardiac blood flow from 4D Flow MRI data using affordable/accessible 3D printers.
2. Evaluating the feasibility of such a framework by physicalizing blood flow data from an actual human heart (specifically the left ventricle (LV)) with different visualization styles.
3. Comparing the usability of the developed physical visualization against conventional digital 3D visualization formats by conducting a user study.

2. Background and related work

The work we present in this paper relates to a few main areas of study: cardiac imaging (specifically, 4D Flow MRI), flow visualization, and physical visualization. This section first provides a broad overview of 4D Flow MRI, and then focuses on 4D Flow MRI data from a scientific visualization perspective, primarily highlighting various qualitative flow visualization techniques. Finally, we broadly present the idea of physical visualization, and highlight some of its current uses in cardiovascular medicine.

There are many cardiovascular magnetic resonance (CMR) imaging techniques [13]. One such technique is 4D Flow MRI (also known as 4D Flow CMR), which can be described as "three-dimensional (3D) cine (time-resolved) phase-contrast CMR with three-directional velocity-encoding" [2]. The captured data encodes flow velocity within a volumetric space in all three spatial directions over time along the cardiac cycle (3D + time = 4D), thus opening up much possibility for understanding flow within the chambers of the heart and great vessels. In light of this technology, a group of physicists, physicians and biomedical engineers came together to produce a consensus paper [2], which provides a summary of many aspects in the 4D Flow MRI workflow, from acquisition to processing. The work we present in this paper fits within the last stage of this workflow, specifically aiming to introduce a novel technique for blood flow visualization.

Processing and visualizing blood flow data has become an area of active interest within the field of computer graphics: a few recent survey papers relating to blood flow visualization [14], data processing of 4D Flow MRI (with a focus on the aorta) [15] and medical flow visualization [16] provide a comprehensive overview of flow visualization in the medical area. Within these surveys, we highlight one main topic related to our work, namely qualitative flow analysis.

Qualitative flow analysis can be broken down into three main categories [15]: (1) direct methods, (2) geometry-based methods and (3) feature-based methods. Direct methods include, e.g. volume rendering of velocity magnitudes, or using line/arrow glyphs to represent the vector field data. Displaying a glyph at each voxel creates visual clutter, so it is common to display vectors with a given distance between each of them, or to only depict vectors within a particular region [17]. These vector displays can be used to qualitatively assess LV inflow/outflow direction, stenotic jet direction, and regions of recirculating flow [17]. Geometry-based flow visualization includes using lines or particles to depict flow. Two of the most common geometry-based techniques used for 4D Flow MRI are streamlines and pathlines: streamlines show the instantaneous nature of the flow, whereas pathlines depict a particle's trajectory in an unsteady flow field over time. A number of methods have been proposed for appropriately seeding and growing these integral lines [12, 18, 19]. These lines can also be interactively seeded (e.g. by selecting vessel cross-sections) [20] and rendered in a stylistic way to improve depiction of the blood flow dynamics [21, 20]. Finally, feature-based methods highlight specific flow characteristics in the data, such as high-velocity jets, vortex cores, or vortex regions. Salzbrunn et al. [22] introduced the idea of line predicates: Boolean functions which indicate if an integral line matches a certain criterion or not. They have been used for bundling flow lines which, e.g. pass through a certain region of interest, are part of a vortex, reach maximal velocity, are a minimum length, or reside in a particular area longer than a specified length of time [23, 24]. Bridging geometry-based and feature-based methods, there has also been work on clustering integral lines to reduce visual clutter, classify flow structures, and aid in physicians'/experts' exploration and understanding of flow data [25, 26, 27, 19]. Software tools which allow the user to clip or slice the data (sometimes creating additional focus windows or inspection lenses [28]) have also been designed in an attempt to decrease the clutter and get a clearer understanding of the data, though the restriction of screen space still hinders comparison between multiple windows.

Despite the advances in flow visualization methods (improved rendering techniques and interactivity, for instance), they are generally still limited to 2D screen displays. As a complementary alternative, there has been recent interest in the area of *physical visualization*. In particular, the work of Jansen et al. [3] highlights the opportunities and challenges for data physicalization. The authors define a data physicalization as "a physical artifact whose geometry or material properties encode data", and discuss numerous benefits of physicalization, such as enabling active perception (e.g. being able to turn a model around or move closer), engaging non-visual senses (e.g. touch, with nuances in perceiving texture, weight, etc.), and bringing data into the real world (the visualization is always "on", which supports casual visualization).

Physical visualization has a broad scope of application. For instance, geospatial data benefits from physicalization by improving interaction and understanding [29, 10]. Even data which we traditionally see in plots and charts can take on a physical form [30, 31, 32]. Herman and Keefe [33] experimented with 3D printing scalar fields on different kinds of surfaces and found that box-shaped glyphs ("boxcars") on spheroids ("potatoes") were most compelling for tangible interaction (users were more likely to pick them up and inspect closer). Bader et al. [34] exploit multimaterial voxel-printing to create physicalizations of 3D data such as volumes from medical imaging, or results from a computational fluid simulation. The example prints are visually striking but require a commercial 3D printer rather than an affordable one. This rather humble sampling of previous work demonstrates the power and profit of physicalizations in a broad sense. However, we are interested in physicalization of *blood flow* specifically and thus now discuss some existing work on physicalization of flow and/or motion in general. Informally, there are a few examples: Allen and Smith [35] artistically 3D printed people's movements in a lobby space over a 10-hour time frame, Langnau [36] reports an example of 3D printing trajectory lines in an engineering application, and Taira et al. [37] explore printing of abstract fluid flow structures. Of note, none of these examples have been studied or presented in a detailed and rigorous way. More formally, there has been work on building software tools for authoring motion geometry [38] and for generating motion sculptures from a series of 2D images [39]. However, both of these studies generally emphasize the portrayal of human motion from a more "macroscopic" perspective (e.g. the movement of a person's limbs while running, or the path swept by a tennis player's swing), rather than a finer, "microscopic" application such as the intricacy of blood flow within the heart. Related to medical data, Acevedo et al. [40] explore the use of expensive colour 3D printing (specifically powder bed fusion) to create diffusion tensor MRI visualization models, employing thick image-based slabs as support. Their initial experiments suggest that physical models enhance usage and analysis of their digital equivalents.

Within the field of medicine, physicalization has manifested itself most commonly in the form of 3D printing [41]. The scope of interest in previous visualization applications mainly focuses on fabricating (patient-specific) anatomical structures. Creating these 3D printed models usually consists of the following steps [4]: (1) acquisition of a volumetric imaging dataset; (2) segmentation of the structure(s) of interest [42], typically with some kind of open source or commercial software; (3) conversion into suitable file format such as STL; (4) 3D printing; and (5) finishing, which includes removing excess support material. This whole process is often rather expensive (both in money and time) [7], which begs the question – what is the benefit of 3D printing medical data versus visualizing it in a traditional way (e.g. with 2D images or using computer software)? Giannopoulos et al. [5] report that fabricated 3D models provide the advantage of haptic feedback, direct manipulation, and enhanced understanding of cardiovascular anatomy and underlying pathologies. Sun and Lee [7] provide a systematic review on cardiovascular 3D printing applications, highlighting findings in three main areas: (1) representing patient data with high diagnostic accuracy, (2) serving as an educational tool for parents, clinicians, healthcare professionals and medical trainees, and (3) using 3D printing as a tool for pre-surgical planning, medical device design, and simulation of diseases. In summary, previous work has investigated 3D printing in numerous medical applications and demonstrated its utility; however, specifically creating a physical representation of blood flow data is a void which we explore in this paper.

3. Slice-based design

The goal of this work is to design a physical representation of blood flow. The blood flow data, obtained from 4D Flow MRI, can be represented as a vector-valued function defined on a subset Ω of $\mathbb{R}^3$ over time, that is,

$$\mathbf{f} : \Omega \times \mathbb{R}^+ \to \mathbb{R}^3. \tag{1}$$

The segmented volume, Ω, is the chamber or vessel of interest; in our work, Ω represents the left ventricle. Determining Ω based on 4D Flow MRI data alone is challenging due to its known low anatomical contrast; therefore, we obtain Ω using an established semi-automated algorithm: the LV is segmented from cine SSFP MRI by manually tracing endocardial contours, then this segmentation is automatically registered to the 4D Flow MRI velocity data by a mutual information algorithm [43]. Note that 4D Flow MRI provides direct in vivo measurements of instantaneous voxel-wise 3D vector field information covering the heart and spanning over the cardiac cycle. Masking the 4D Flow data with the registered LV segmentation provides us with the input data to our system: a given subject's blood flow data within the LV at snapshots in time over the cardiac cycle (for each snapshot, $\mathbf{f} : \Omega \to \mathbb{R}^3$).

Given this input, we are faced with a challenging question: how does one convert volumetric flow data into a fabricable model? To begin, we decided to target two styles of visualization that are relatively common in traditional flow visualization: (1) glyphs, which represent the "raw" vector field data, and (2) streamlines (a type of integral line), which portray the flow character at a snapshot in time. A glyph, for our usage within the context of this paper, is a visual symbol or representation of a vector at a given point in space. Perhaps the most common glyph used for vectors is an arrow, as it naturally encodes the concept of direction. The orientation of the glyph at a point $p \in \Omega$ can be defined using $\mathbf{f}(p)$. A streamline is an integral curve $s(\tau) = (x(\tau), y(\tau), z(\tau))$ which is tangent to the vector field everywhere (τ parameterizes the curve). That is, it satisfies the following:

$$\dot{s}(\tau) = \mathbf{f}(s(\tau)), \tag{2}$$

with the initial condition $s_0 = s(0)$. This initial condition is often called a *seed*, which is some point in space within the vector field ($s_0 \in \Omega$). To calculate a streamline in practice, we begin with a seed point and trace it through the vector field using some kind of numerical integration technique (such as Euler or Runge-Kutta integration). Ultimately, we find a number of points along the streamline curve which we use to represent that streamline; this set of points we denote with S.

Both vector glyphs and streamlines are usually thin and disparate, making them challenging to 3D print. To overcome this complication, we drew from physicians' typical use of cross sections or "slices" to acquire and explore medical image data [11]. Thus we arrive at the concept of our proposed design: slice-based physical visualization. The core idea is to use slices of the segmented volume Ω (Fig. 3) as a natural support structure, which alleviates some of the core difficulties in 3D printing (e.g. supporting floating structures/objects, fragility of thinner features, etc.), while also providing some contextual cues (since the shape of the slice represents a cross section of the segmented volume). In addition, the slices can be spaced out such that the slicing frequency is suitable for the desired visualization – the number of slices can be as many or as few as preferred for a given dataset. Note that "slices" here refer to thin slabs (subsets of Ω), as an extremely thin 2D plane would be nearly impossible to 3D print.

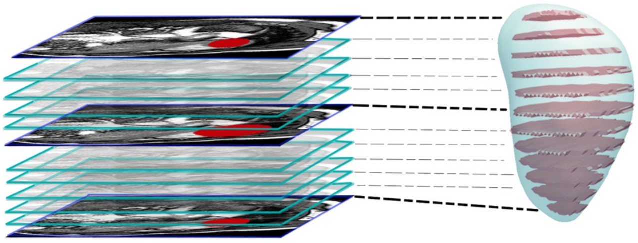

Fig. 3. The LV (highlighted in red in the short axis images on the left) can be segmented from MR image data (a stack of 2D slices which make up a 3D volume). Such a segmentation represents the chamber's volume. For physicalization, this volume can be "sliced" into thin slabs (shown on the right), which provide a natural support structure for physicalization while also maintaining a sense of the data.

We applied this conceptual design to both types of flow representations – vector field glyphs and streamlines – using segmented LV 4D Flow MRI data. The next two sections (Sections 4 and 5) will describe each of these models in more detail, including their construction and fabrication. Following that, Section 6 describes the user study procedure and results, and Section 7 discusses design improvements and physicalization in the context of blood flow data.

4. Glyph model

The basic idea of our glyph model is to represent the data points in the LV and their associated vectors with some directional glyphs. However, representing every data point (in a Cartesian grid with 1.57 x 1.32 x 4.43 mm^3 spacing) with a glyph would result in an extremely cluttered model, not to mention the high likelihood of failure to print. Hence, only a subset of the data should be chosen. We select that subset using the slice-based design idea: each slice is a thin slab which represents some subset of the vector field data. Data points contained within each of these thin volumes are candidates for the final model; however, converting every data point even within these thin slabs will still result in many overlapping glyphs. Consequently, we keep every nth data point ($n = 10$ for our example models) to convert into a directional glyph. Our goal was to strike a balance between comprehensiveness and comprehensibility – we want enough slices to represent the flow in its entirety (comprehensively), while limiting cognitive overload and visual clutter (comprehensibly). To do this, we also chose to evenly space the slices (for improved aesthetic quality), and to linearly scale the glyphs to prevent inter-slice collisions.

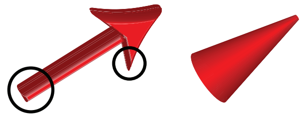

Fig. 4. Arrow glyphs have small, fragile parts (circled in black), whereas cones can portray directional information but are not as breakable.

In addition to slicing, selecting an appropriate glyph required particular consideration. As observed in Fig. 4, arrow glyphs – while common for 2D vector field visualizations – are challenging to print. Thin arrow tails break easily once fabricated, and do not provide adequate support for the arrowhead. This is unfortunate, since arrows can clearly encode direction as well as potentially another variable (e.g. vector magnitude can be shown with the size of the arrow). Based on these desirable attributes, the most natural alternative glyph was a cone. Cones are similar in shape to arrows and can likewise portray direction and speed based on orientation and scaling, but are more printable since they do not have fragile features. Once the glyphs are embedded into a slice, a collection of glyphs becomes much easier to print. Moreover, scaling the glyphs based on vector magnitude gives a clear impression of the predominant flow direction (Fig. 5).

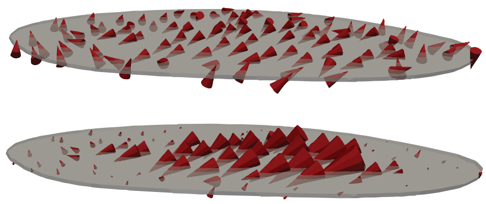

Fig. 5. Cone glyphs are embedded within a slice for printability. Unscaled glyphs (top) only show the direction of the vectors whereas scaling the glyphs based on vector magnitude (bottom) give a distinct impression of the primary flow direction (jet).

4.1. Physicalization of relative and anatomical context

The slice-based model described so far accounts for many of the challenges associated with affordable 3D printing, but a collection of mere slices won't hold up in the real world – however nice a virtual model may seem, once physicalized it must stand the test of gravity. Therefore, some additional design considerations were necessary.

Firstly, we needed some additional physical parts which would support the model's existence in the real world without losing spatial context (i.e. the position of one slice relative to another). We achieved this by designing slice handles and a stand with a wheel and axle-type mechanism (Fig. 6). The base, a rectangular prism with a small cylinder, holds a vertical post. The vertical post, in turn, holds the slices of the model: a "handle", made up of a thin rectangular piece and a hollow cylinder, is affixed to each slice, and each cylinder can be slid onto the vertical post. The cylinder heights are designed such that the spatial relationships between slices are preserved. Although this design is relatively simple, it includes some important features: the relative spatial positions of the slices are maintained, and having the post inside each handle cylinder (similar to a wheel and axle) allows for rotation and inspection of individual slices while preserving contextual awareness.

Secondly, we wanted to provide some basic anatomical context by creating a representation of the LV's endocardial layer. Generation of the LV shape was kept simple: the data had already been segmented (based on endocardial contours), so we formed a surface from the volumetric data itself (i.e. Ω). Because the voxels were relatively coarse, smoothing was applied. Since the anatomical structure is not the main focus of this visualization, we did not want it to impede interaction with the flow model; therefore, the surface was cut using a plane to form a "half-shell" shape. To 3D print the surface, it was also necessary to add some thickness to the model, which was achieved by extruding 2mm along the surface normals. Finally, the anatomical context was embedded into the base, thus completing the physical model (Fig. 6).

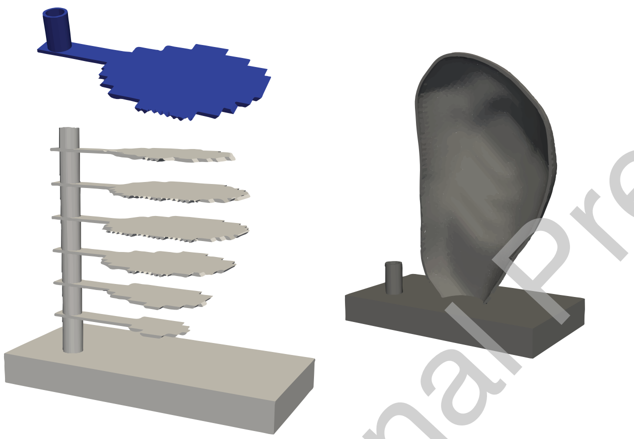

Fig. 6. Each slice model includes a supplementary handle (shown in blue, top left), which allows for easy assembly into a stack of slices (bottom left). The LV anatomical shell is attached to the rectangular base (right).

4.2. Fabricated glyph model

Two glyph models were created from two datasets (i.e. two time frames), both derived from a 4D Flow MRI scan of one healthy subject. The models were printed using the MakerGear M2. Because the cone glyphs were embedded in each slice and could appear on either side of the slice (Fig. 5), we printed each slice model in halves and then glued the slices together. This prevented the need for additional support material. The final physical models were completely 3D printed except for the vertical post used to support the slices; we used a wooden dowel for this post. Spacing between slices was approximately 12 mm and the thickness of each slice was 2 mm.

Although an individual fabricated model represents a single snapshot in time, we wanted to incorporate the idea of time-varying data as well. For this, we acknowledge the importance of key events in the cardiac cycle [44]; for example, during ventricular diastole, there is *early filling* (when the ventricles relax and blood flows in from the atria due to pressure difference) and *late filling* (when the atria contract and push blood into the ventricles). Thus, our two models represent key time frames, which aligns with common practice in medical textbooks and research publications. Since our focus was the LV, we chose to use early filling and late filling. Both models were sliced with the same spacing so that the slices would be comparable (Fig. 7). To get a finer sense of the flow evolution over time, one could print each time frame in between, similar to how LAIKA studio creates models for stop-motion animation [45].

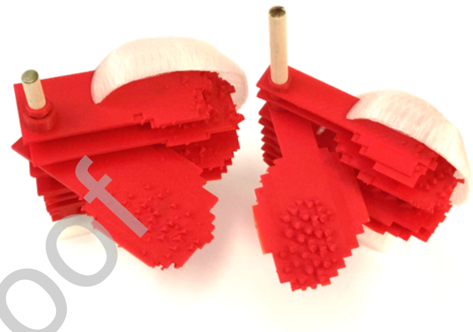

Fig. 7. Picture of fabricated LV late filling (left) and early filling (right) vector field glyph models; both are sliced such that corresponding slices can be compared between the two.

5. Streamline model

Although representing the raw vector field may be the most faithful to the original data, it might not be the easiest to interpret. For this reason, we also developed a method for creating a physical streamline model. However, producing a physicalizable streamline representation is not simple: careful thought must first be given to how the streamlines are seeded, and once the streamlines are formed, each of them must be converted into a mesh which can be 3D printed.

5.1. Generating streamlines

When generating streamlines, one is always faced with competing goals. Tracing many streamlines can reveal interesting flow characteristics, such as areas of vortical flow, sources, sinks, saddles, etc. Unfortunately, a large number of streamlines quickly clutters the visual field, ultimately obscuring whatever feature(s) we originally intended to discover. To manage these competing goals, we adopted the idea of generating streamlines using a *similarity-guided* placement strategy [12], as this technique reportedly achieved a balance between uncovering interesting flow behaviour and limiting visual clutter.

The streamlines generated by this method [12] have some natural spacing (a minimum Euclidean distance between lines) to reduce clutter and occlusion, but also represent interesting features in the flow. Streamlines with similar trajectory are reduced in number, whereas streamlines with distinct directions and shapes are more likely to be preserved in the final visualization. Chen et al. [12] define similarity distance between a point p on a growing streamline S_i to another (existing) streamline

S_j (Fig. 8). The closest point q on S_j is found and two sample windows of the same size are formed, one about point p and the other about point q, which are then uniformly sampled with m samples along the streamline. If a symmetric window cannot be formed about one or both points p and/or q (e.g. the point is at the end of a streamline), one-sided windows are used instead. Once these two sets of sample points have been formed, the similarity distance is calculated [12]:

$$d_{sim} = \|p - q\| + \frac{\alpha}{m} \sum_{k=0}^{m-1} \big|\|p_k - q_k\| - \|p - q\|\big| . \tag{3}$$

The more *distinct* two streamlines are, the greater the similarity distance between them. A new streamline S_i which has a large similarity distance between all existing streamlines indicates that S_i should be included in the final visualization.

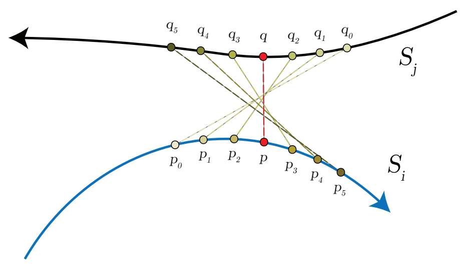

Fig. 8. The similarity distance is measured in a local neighbourhood at the point p where the streamline S_i is growing.

To obtain a set of streamlines for physicalization, seed point locations are initialized in a Cartesian grid covering the volume and each streamline is traced (both forwards and backwards) using the Runge-Kutta-Fehlberg (RKF45) method [46]. Growing a given streamline is stopped if it is too similar to an existing streamline ($d_{sim} < d_{min}$) or too similar to itself ($d_{sim} < d_{self}$). When comparing the final set of streamlines to a set of streamlines created without any filtering, the number of streamlines generated using the similarity-guided strategy is at least 90% less (e.g. 646 lines vs. 59 lines), but the overall flow behaviour is still captured (Fig. 9). Furthermore, the user-established thresholds (e.g. d_{min} and d_{self}) offer flexibility when creating a printable set of streamlines; for example, they can be customized to suit a specific 3D printer's resolution.

5.2. From lines to meshes

Once a set of streamlines has been generated, it is necessary to convert it into a mesh for 3D printing. We used sweep surfaces to accomplish this task. A cross section shape is selected and "swept" along each streamline (trajectory curve), adjusting its orientation using the parallel transport approach [47]. For simplicity, we used a circular cross section since it generates a tube (Fig. 10), which is a natural three-dimensional extension of a line; however, any arbitrary 2D curve could be used. We used a cross section diameter of 3 mm to ensure printability, at the cost of some overlap with voxels surrounding the streamline. Specifically, a given cross section might partially overlap with at most 9 voxels based on the spatial resolution of the data, though we would expect a typical overlap of 2-4 voxels.

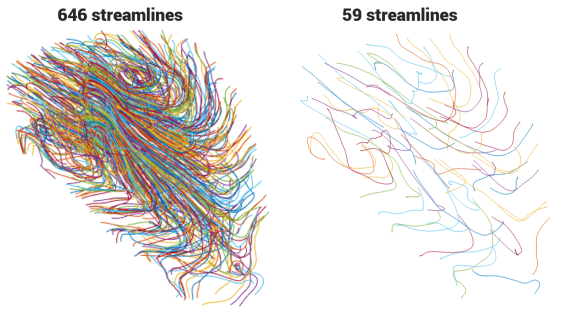

Fig. 9. Naïvely growing all streamlines for a given set of seed points results in a very cluttered visualization (left), whereas applying the similarity distance metric when generating the streamlines from the same seed points results in a cleaner, physicalizable collection (right).

Many previous streamline visualizations do not seem to include directional information [18], making the overall character of the flow somewhat ambiguous. Therefore, we enhance our model by adding conical arrowheads at the end of each tube. These were constructed by interpolating the vector field at the endpoint of each streamline ($\mathbf{v}_i$) and attaching a cone whose axis aligns with $\mathbf{v}_i$ (Fig. 10).

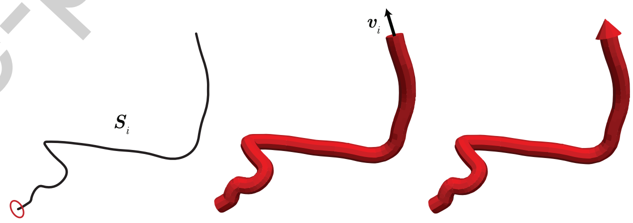

Fig. 10. We build each streamline mesh by sweeping a circular cross section along the streamline (left). Rather than having an ambiguous streamline mesh (middle), we add a conical arrowhead (right) to indicate the direction of the streamline.

After obtaining a complete set of streamline meshes, we apply our proposed slicing method to provide intermediate support for the streamlines (see Section 4.1). Slicing reduces the total amount of support material required and allows for assembling into a model that maintains the overall shape of the streamlines. Unlike the vector field model, the streamlines do not need to be embedded in the slice. Consequently, we chose to use fewer slices than the vector field model: too many slices in the streamline model becomes obtrusive, as they interrupt the shape of any streamline spanning multiple slices.

5.3. Fabricated streamline model

The final model was printed using the MakerGear M3-ID. One advantage of the M3-ID over the M2 is that it is equipped with two extruders, making it possible to print with two colours in the same model. We leveraged this by using a translucent filament for the slices and support material, and using a red filament for the streamlines themselves. This highlights the streamlines compared to the slices, support, and base, thus emphasizing the flow features in the model (Fig. 11). To assist with inspection of the data, the model was scaled up 1.5x in all dimensions within Simplify3D. The complete streamline model was fabricated with a total print time of approximately 1.4 days and required about 330 grams of PLA filament. In the printed model, spacing between slices was approximately 22 mm and streamline radii were 2.25 mm each.

Fig. 11. Picture of the printed LV streamline model (early filling).

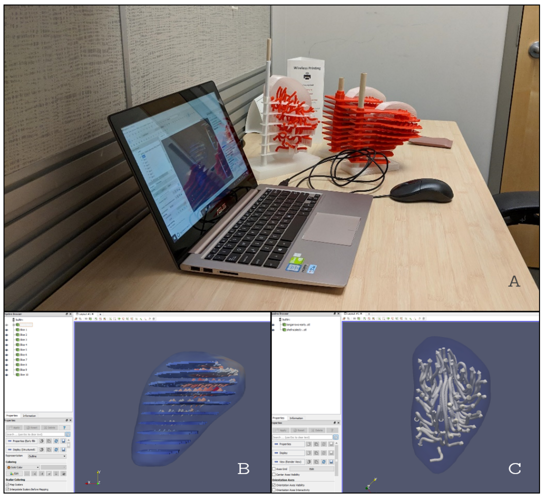

Fig. 12. (A) User study setup, with screenshots of corresponding digital visualizations for (B) the glyph models and (C) the streamline model.

6. User study

We conducted a user study to evaluate our physical visualization prototypes. The goal of the study was to discover how people would interact with the physical visualization models, and to see how they differ with respect to comparable digital visualizations (specifically using a freely available, conventional scientific visualization software, Paraview [48]). We had 16 subjects (8 male, 8 female) who participated in the study, all of whom had some prior medical training/knowledge. Fourteen participants were second-year medical students (all with varying prior backgrounds), one was a family medicine resident and one was a general internal medicine doctor.

6.1. Procedure

Users had the opportunity to view and interact with the physical models (two vector field glyph models and one streamline model), as well as comparable digital models of each (see Fig. 12) during the three phases of the study: (1) tasks, (2) post-task questionnaire/survey, and (3) qualitative interview. A brief description of the basic interaction controls (i.e. rotating, panning, and zooming in/out using a mouse) for Paraview was provided as none of the participants had prior experience with Paraview.

For the task phase, users were asked to complete three different tasks. Tasks marked with * indicate *comparative tasks*, which were executed once using the appropriate physical model and once using the corresponding digital model.

1. Between two slices of the vector field glyph model, determine which has the higher flow magnitude. *
2. After viewing and interacting with both physical and digital streamline models, select one and use it to briefly describe what you see happening in the flow.
3. Compare two streamlines (as identified by the experimenter) and report which one you believe is closer to you, using your initial viewpoint as a reference. (Users are allowed to interact with the model.) *

The post-task questionnaire had four statements which were ranked on a scale from 1-5 (1-strongly disagree, 3-neutral, 5-strongly agree) for each of the four visualization types (physical glyph model, digital glyph model, physical streamline model, and digital streamline model). The first three statements were the same for all visualizations, the last statement differed only between glyph/streamline models:

1. The visualization was clear and easy to understand.
2. The visualization was easy to interact with.
3. It was easy to see/navigate different parts of the data.
4. The interaction technique allowed me to easily *compare different parts of the data* (glyph models) / *understand the shape and direction of the data* (streamline models).

Finally, the user study concluded with three questions in the interview phase:

1. In general, what do you think of working with physical models vs. digital models?
2. What is your overall opinion about physical visualization?
3. What do you think of the physical glyph model vs. streamline model?

6.2. Results

When comparing slices using the glyph models (Fig. 13, top), users were generally faster when using the physical model over the digital version of the same (statistical p-value = 0.031). Based on the scores of the post-task questionnaire, it appeared that users generally favoured the digital glyph models over the physical models (average score of 17 vs. 16.25); however, this difference was not statistically significant (p-value = 0.150). Given these results, we consider the physical glyph model to be at least comparable to a digital representation, with the advantage of enabling faster comparisons between slices.

As for the streamline models, slightly more participants (10 of 16) chose to use the digital version to describe the flow behaviour, rather than the physical. Those who chose the physical

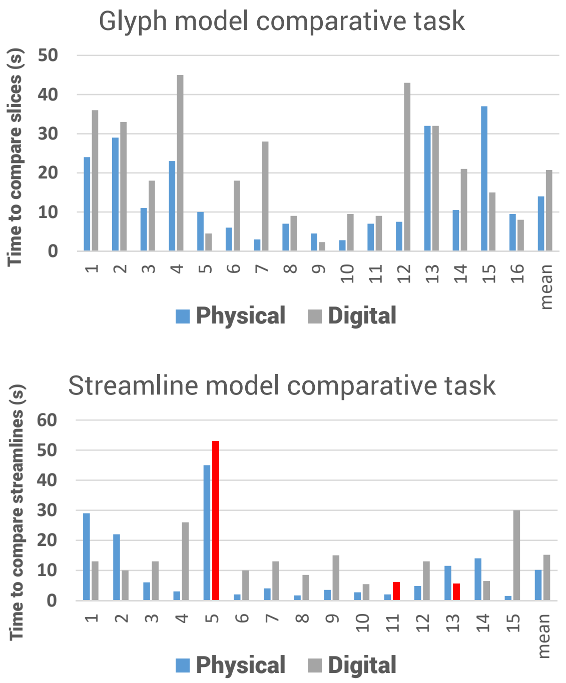

Fig. 13. For both the glyph model comparative tasks (top) and the streamline model comparative tasks (bottom), most users were faster using the physical model (blue) over the digital model (grey). Three users chose the incorrect streamline when working with the digital model (red).

model tended to gesture with their hands while describing the flow. Regardless of which model was chosen, all participants described some aspect of the flow accurately. For the comparative task, it appeared that majority of participants were faster using the physical model over the digital (Fig. 13, bottom) but this was not considered statistically significant at the 5% significance level (p-value = 0.062). (Only 15 participants' data were used since one participant's records of working with the streamline models were partially lost due to equipment malfunction.) However, perhaps more importantly, depth perception *accuracy* was 100% when using the physical model, as opposed to 80% when using the digital model. This supports the idea of physical visualization enabling better, more natural depth perception. In terms of the questionnaire results, although more users ranked the digital streamline visualization higher than the physical (average scores of 16.25 and 15.22 respectively), this difference was not statistically significant either (p-value = 0.096).

Overall, the results related to the streamline models seemed inconclusive; there was no distinct advantage of physical over digital or vice versa. Nonetheless, this user study gave us some key insight into our physical streamline model design. We had originally hypothesized that the intermittent slices (which necessarily split most streamlines over at least two sections) would not interfere with perceiving each line as a whole. This hypothesis was based on the ideas of Gestalt theory [49], which suggest that people tend to understand things as a whole rather than as individual parts. But, at least three participants mentioned that they found the slices obtrusive and/or that the lines were difficult to follow through the model. Since there are quite a number of lines, it makes sense that the cognitive demand of interpreting the lines within each slice and simultaneously trying to combine the lines between slices would be quite high.

During the interview phase, majority of participants expressed appreciation for both physical and digital models. Some noted that they found manipulation easier with the digital model (e.g. being able to rotate freely) while handling the physical model was less fluid due to the stand design. Others mentioned that they appreciate the tangibility of physical models and indicated its particular usefulness for "hands-on" learners. The idea of physical size was also highlighted during the interview phase; at least seven of the participants noted the importance of understanding real-world scale using physical models, which is a difficult concept to grasp digitally (since most manipulation methods allow for easy zooming in and out).

Two participants mentioned lack of portability as a drawback to using physical models in the context of healthcare. However, a different participant (who had previous experience working in pediatrics) liked the idea of interacting with patients using a physical model over a digital one. This participant described prior experience of using a laptop with children: the presence of a laptop would often introduce distraction to children who simply wanted to play video games. Furthermore, the participant anecdotally explained their frustration with technology that would sometimes fail to work; this experience resonates with the idea of physical visualizations being always "on". Another participant believed that physical models would have less of a learning curve, especially for those who are not technologically inclined.

7. Design improvements and discussion

Physicalization of medical blood flow data has been largely unexplored up to this point, but based on the proof-of-concept we present, we believe that it is an area with interesting possibilities. In this section, we describe further design improvements based on the feedback from the user study, followed by a summary of informal discussions with medical experts that took place after the updated streamline model was developed. From this feedback, we present two more examples of physical flow models. Finally, we apply our methods to a patient's dataset, demonstrating the use of physical visualization as a tool for exploring abnormal flow patterns.

7.1. Two colour glyph model

During the user study, a few participants mentioned that it would be nice if the glyphs and slices had distinct colours. This was not possible using the MakerGear M2 since it has a single extruder, but it is possible with the M3-ID. A sample long-axis slice was printed to illustrate the potential (Fig. 14).

7.2. Single slice streamline model

Using the results and observations from our user study, we decided to revisit the slice-based design of the streamline model. In particular, we wanted to know if there was an alternative set of slices that could adequately support the streamlines but with less obstruction of the streamline data. During the

Fig. 14. Printed glyph model (long-axis slice) using a dual extrusion printer.

user study, we also noticed that the wheel-and-axle construction seemed more natural when handling the glyph model (e.g. for comparing slices or inspecting a specific subset of data); the idea of comparison between slices using the streamline model is not that valuable. The slice(s) in the streamline model primarily provide support and anatomical/data context.

In light of this, we decided to use a single slice design. We chose a slice that approximates a long-axis cross sectional view, since it is one of the basic cardiac imaging views. Additionally, it has a relatively large cross sectional area, which provides enough support for the streamline structures. Once printed and assembled (Fig. 15), the model can be handled with relative ease. Furthermore, the long-axis slice combined with the overall extent of the streamlines seem to provide sufficient anatomical context, so no additional stand or structures were printed. By creating a somewhat irregular shape (akin to a "potato") we hope to encourage user interaction with the model – picking it up, inspecting it, etc. [33]. The user study also elucidated the benefit of physical scale, so we ensured that the single slice streamline model was printed to scale.

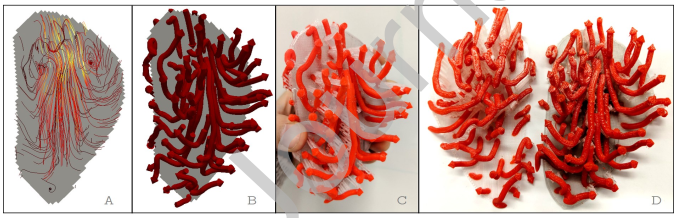

Fig. 15. Screenshots from Paraview showing (A) unfiltered streamlines (generated within Paraview), and (B) the filtered streamline model for printing. Pictures of the fabricated single slice LV streamline model in (C) its final form, and (D) printed in two halves.

7.3. Expert feedback

After developing the single slice streamline model, we received some feedback from four medical experts, primarily radiologists (three experts in cardiac MRI and one surgeon). Although some of the more senior radiologists did not feel that a physical representation was necessary (after many years of experience, they felt that they could adequately reconstruct 3D geometry from 2D images in their minds), some of the radiologists specifically involved with pediatrics expressed interest in having physical models to complement digital visualizations. This aligns with the user study results and supports the idea of using physicalization, particularly for pediatric applications. One expert also noted that more simplified models would also be useful.

7.4. Summary models

Our original glyph and streamline models aimed to be as comprehensive as possible, without becoming overly cluttered. This comes from the mindset of representing as much data as possible. However, expert feedback suggests that another approach would also be useful, i.e. creating more simplified flow models. We explore this idea with two example cases: a pathline predicate model, and a vortex core model. Both of these can be considered as "summary models", designed to give a simplified overview of (some aspect of) blood flow character over the cardiac cycle.

7.4.1. Pathline predicate model

Pathlines are integral lines, very similar to streamlines, which are derived for time-varying, unsteady vector fields. A pathline is often described as the trajectory that a massless particle would follow in the flow field over time. As such, a pathline $p(t)$ is defined similarly to a streamline (Eq. 2) but is parameterized by t (physical time) rather than τ. We create an initial set of pathlines $\mathcal{P}$ as follows: we use the same spatial seeding strategy described in Section 5 at $t = 0$, then we trace pathlines from the seeds over the cardiac cycle ($t \in [0, t_f]$) using RKF-45 [46]. Note that $t = 0$ represents early diastole and $t = t_f$ corresponds to end systole.

The set of pathlines, $\mathcal{P}$, is likely to be dense, confusing, and nearly impossible to 3D print. As with glyphs and streamlines, minimizing clutter is always desirable and pathlines are no exception. Moreover, the goal of this model is to create a summarized depiction of the flow and should arguably be even less cluttered than the glyph and streamline models. Hence, to filter $\mathcal{P}$ into a printable and simplified set of pathlines, we chose to use *pathline predicates*. Pathline predicates [22, 24] are Boolean functions which can classify and filter pathlines based on user-defined attributes (e.g. residence time, maximum velocity, passing through a region of interest, etc.). Combining different predicates using Boolean logic allows users to answer questions, such as "which pathlines pass through a particular region and have the highest speed?". For our example pathline predicate model, we decided to ask the question "which pathlines have the highest speed and are the longest?", thus combining a predicate for maximal speed (at some point along the pathline) and length. We define our predicates based on the *length* and *maximum velocity* predicates described by Jankowai et al. [24].

Thus far, our physical models have represented flow behaviour at a snapshot in time. However, since pathlines are derived from time-varying data, the physical model can be designed to reflect this. We modified our sweep surface algorithm (Section 5.2) such that the cross-sectional radius is linearly scaled based on the time that the "particle" has travelled along the pathline. This gives the pathtube a tapered appearance, suggesting the idea of movement over time; these are similar to motion lines which are common in traditional comic book art [50].

By leveraging the single slice technique described in Section 7.2, we create a physicalizable pathline predicate summary model (Fig. 16). The summary print has only ten pathlines but provide an overview of the predominant flow behaviour – for instance, three of the pathlines are seen merging into one general direction, corresponding to ejection during systole.

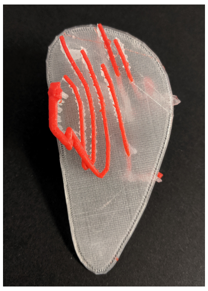

Fig. 16. Picture of 3D printed pathline predicate model for a healthy subject.

7.4.2. *Vortex core model*

Up to this point, we have focused on some of the fundamental flow/vector field visualization techniques, such as glyphs and integral lines. However, there are also a number of flow-related features and hemodynamic parameters, such as pressure, wall shear stress, etc. One feature that has garnered particular interest within the context of blood flow in recent years is *vortical flow* [51, 52, 53]. Pedrizzetti et al. [51] suggest that maladaptive intracardiac vortices may be involved in LV remodelling and could provide early indications of long-term outcomes. As such, vortex cores seemed to be a suitable flow feature worth exploring in the context of cardiac blood flow.

Robust vortex extraction is a challenging problem, with a formal definition of a vortex still lacking [54]. Numerous methods for vortex core detection have been proposed [54]; the method presented by Jeong and Hussain [55] known as the λ_2 method, is generally regarded as the most suitable for vortex core extraction for blood flow in the cardiovascular system [52]. Therefore, we chose this method for vortex core extraction.

We extract vortex cores during early diastole using the λ_2 method [56], and subsequently convert the vortex core voxels into surfaces for 3D printing. The long-axis single slice technique described in Section 7.2 is again suitable for supporting the 3D printed vortex core structures (Fig. 17). Moreover, a summary trajectory line (e.g. a pathline derived from a combination of various predicates, such as seeding plane, maximum velocity and/or length) to provide time-varying information can be included in the physical vortex core model. Since it is not the focus of the visualization, it can be projected onto the slice plane, acting as part of the model's context.

7.5. *Patient example*

To further test our improved designs, we applied them to a dataset of a patient with cardiomyopathy (a disease of the heart muscle). Fig. 18 shows comparisons between the healthy subject and patient using three of the different flow models (streamlines, pathline predicates and vortex cores). In Fig. 18A, the

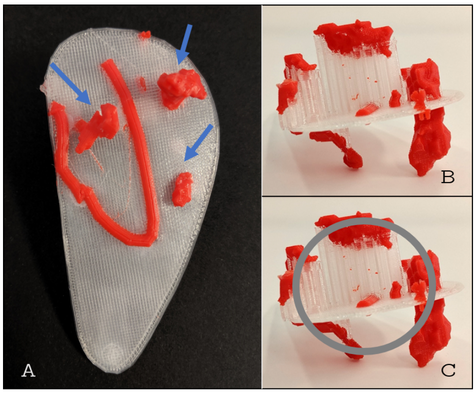

Fig. 17. Pictures of healthy vortex core summary model. (A) Long-axis view, with vortex cores marked by arrows. (B) Short-axis view, a vortex core ring structure (C) can be observed.

difference in streamline flow pattern structure show the disorganized flow in the patient's LV during early filling when compared to the healthy subject. Fig. 18B shows that a greater proportion of blood flow enters/exits the LV within one cardiac cycle in the healthy subject as compared to the patient, suggesting that the healthy subject can transport oxygenated blood more efficiently. Finally, in Fig. 18C, an early vortex ring-like structure can be seen in both cases but the vortex core structure of the patient is not as well-formed. Hence, these examples show the potential of using physicalization to portray the hemodynamics of different cases.

8. Implementation

For creating the glyph models, a macro was written in Paraview to automatically generate the slice-based model with user-specified orientation, slice spacing, and glyph size scaling (to prevent collisions between slices). Meshmixer was used for building the handles and base, as well as for ensuring that the models would be 3D printable (i.e. having no open boundaries). To print, we used Simplify3D for automatically generating support structures and gcode (instructions for the printer) and MakerGear's M2/M3-ID printers with AMZ3D PLA filament. The programs for creating the streamline, pathline and vortex core models were implemented in MATLAB (R2016a).

9. Conclusions and future work

4D Flow MRI is an exciting technology which captures volumetric blood flow data over time and has much potential for both research and clinical use. One of the important pieces of the 4D Flow MRI processing pipeline is flow visualization, which can help various users (e.g. doctors, patients, researchers, students, etc.) better understand the data. There are many ways to visualize flow data, including vector field maps, integral lines, and feature-specific displays. However, to truly grasp the three-dimensional (or four-dimensional, when considering time) nature of the data, it may be beneficial to explore it using a tangible three-dimensional visualization. To this end,

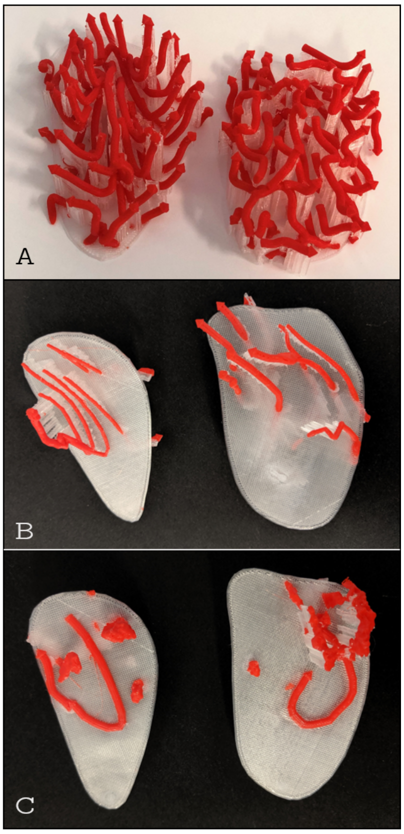

Fig. 18. Comparison between LV of healthy subject (left) to cardiomyopathy patient (right) in photos of (A) two printed streamline (half-)models, (B) pathline predicate models, and (C) vortex core summary models.

we designed a novel slice-based physicalization method for visualizing 4D Flow MRI data, specifically focusing on blood flow within the left ventricle.

Overall, this study provides a proof-of-concept on the feasibility of a novel physical visualization of blood flow within an actual human heart. We demonstrate that our proposed slice-based design is easily fabricable, and has the potential to be useful for physicalizing blood flow data. Since this area has not yet been extensively explored, we initially focused on two styles of visualization, glyphs and streamlines: one can consider glyphs as the lowest level of visualization since they most closely correspond with the raw vector field data, and streamlines can be thought of as one level higher, being derived from the vector values in space. Beyond these two styles, we explore two simplified summary model designs, which represent the time-varying aspect of the data as well. These models could have utility in patient/trainee education, which we hope to study in more depth (e.g. with longitudinal user studies).

While our presented workflow (as-is) is not intended for *routine* clinical use, it provides a tool for research applications, particularly in studies which utilize 3D printing. As an example, specific flow features (for instance, regurgitant flow) could be modelled to complement other anatomical 3D prints, thus augmenting structural information with hemodynamics. Various clustering techniques have been applied to 4D Flow streamline data [25, 26]; these could be used to create more simplified flow overviews for physicalization as well. We hope to investigate such future designs in collaboration with clinical experts, tailored to potential use cases and audiences (e.g. pediatrics).

Acknowledgments

(Placeholder for acknowledgements section)

References

[1] Markl, M, Frydrychowicz, A, Kozerke, S, Hope, M, Wieben, O. 4D flow MRI. Journal of Magnetic Resonance Imaging 2012;36(5):1015–1036.

[2] Dyverfeldt, P, Bissell, M, Barker, AJ, Bolger, AF, Carlhäll, CJ, Ebbers, T, et al. 4D flow cardiovascular magnetic resonance consensus statement. Journal of Cardiovascular Magnetic Resonance 2015;17(1):72.

[3] Jansen, Y, Dragicevic, P, Isenberg, P, Alexander, J, Karnik, A, Kildal, J, et al. Opportunities and challenges for data physicalization. In: Proceedings of the 33rd Annual ACM Conference on Human Factors in Computing Systems. CHI '15; New York, NY, USA: ACM. ISBN 978-1-4503-3145-6; 2015, p. 3227–3236.

[4] Farooqi, KM, Cooper, C, Chelliah, A, Saeed, O, Chai, PJ, Jambawalikar, SR, et al. 3d printing and heart failure: The present and the future. JACC: Heart Failure 2019;7(2):132 – 142.

[5] Giannopoulos, AA, Mitsouras, D, Yoo, SJ, Liu, PP, Chatzizisis, YS, Rybicki, FJ. Applications of 3D printing in cardiovascular diseases. Nat Rev Cardiol 2016;13(12):701–718.

[6] Rengier, F, Mehndiratta, A, von Tengg-Kobligk, H, Zechmann, CM, Unterhinninghofen, R, Kauczor, HU, et al. 3d printing based on imaging data: review of medical applications. International Journal of Computer Assisted Radiology and Surgery 2010;5(4):335–341.

[7] Sun, Z, Lee, SY. A systematic review of 3-d printing in cardiovascular and cerebrovascular diseases. In: Anatolian Journal of Cardiology. 2017,.

[8] Li, J, Li, P, Lu, H, Shen, L, Tian, W, Long, J, et al. Digital design and individually fabricated titanium implants for the reconstruction of traumatic zygomatico-orbital defects. The Journal of craniofacial surgery 2013;24 2:363–8.

[9] Matsumoto, JS, Morris, JM, Foley, TA, Williamson, EE, Leng, S, McGee, KP, et al. Three-dimensional Physical Modeling: Applications and Experience at Mayo Clinic. RadioGraphics 2015;35(7):1989–2006.

[10] Allahverdi, K, Djavaherpour, H, Mahdavi-Amiri, A, Samavati, F. Landscaper: A Modeling System for 3D Printing Scale Models of Landscapes. Computer Graphics Forum 2018;.

[11] Tietjen, C, Meyer, B, Schlechtweg, S, Preim, B, Hertel, I, Strauß, G. Enhancing slice-based visualizations of medical volume data. In: Proceedings of the Eighth Joint Eurographics / IEEE VGTC Conference on Visualization. EUROVIS'06; Aire-la-Ville, Switzerland, Switzerland: Eurographics Association. ISBN 3-905673-31-2; 2006, p. 123–130.

[12] Chen, Y, Cohen, J, Krolik, J. Similarity-guided streamline placement with error evaluation. IEEE Transactions on Visualization and Computer Graphics 2007;13(6):1448–1455.

[13] Tseng, WY, Su, MY, Tseng, YH. Introduction to Cardiovascular Magnetic Resonance: Technical Principles and Clinical Applications. Acta Cardiol Sin 2016;32(2):129–144.

[14] Vilanova, A, Preim, B, van Pelt, R, Gasteiger, R, Neugebauer, M, Wischgoll, T. Visual Exploration of Simulated and Measured Blood Flow; chap. 25. Mathematics and Visualization; Springer-Verlag London; 2014, p. 305–320. ISBN 978-1-4471-6497-5.

[15] Khler, B, Born, S, van Pelt, RFP, Hennemuth, A, Preim, U, Preim, B. A Survey of Cardiac 4D PC-MRI Data Processing. Computer Graphics Forum 2016;36(6):5–35.

[16] Oeltze-Jafra, S, Meuschke, M, Neugebauer, M, Saalfeld, S, Lawonn, K, Janiga, G, et al. Generation and Visual Exploration of Medical Flow Data: Survey, Research Trends and Future Challenges. Computer Graphics Forum 2018;:to appear.

[17] van der Geest, RJ, Garg, P. Advanced Analysis Techniques for Intracardiac Flow Evaluation from 4D Flow MRI. Curr Radiol Rep 2016;4:38.

[18] McLoughlin, T, Laramee, RS, Peikert, R, Post, FH, Chen, M. Over Two Decades of Integration-Based, Geometric Flow Visualization. Computer Graphics Forum 2010;.

[19] Yu, H, Wang, C, Shene, CK, Chen, JH. Hierarchical streamline bundles. IEEE Transactions on Visualization and Computer Graphics 2012;18(8):1353–1367.

[20] van Pelt, R, Bescos, JO, Breeuwer, M, Clough, R, Groeller, ME, ter Haar Romeny, B, et al. Exploration of 4D MRI blood-flow using stylistic visualization. IEEE Transactions on Visualization and Computer Graphics (Proc IEEE Visualization) 2010;16(6):1339–1347.

[21] Lawonn, K, Gnther, T, Preim, B. Coherent View-Dependent Streamlines for Understanding Blood Flow. In: Elmqvist, N, Hlawitschka, M, Kennedy, J, editors. EuroVis - Short Papers. The Eurographics Association. ISBN 978-3-905674-69-9; 2014,.

[22] Salzbrunn, T, Garth, C, Scheuermann, G, Meyer, J. Pathline predicates and unsteady flow structures. Vis Comput 2008;24(12):1039–1051.

[23] Born, S, Markl, M, Gutberlet, M, Scheuermann, G. Illustrative visualization of cardiac and aortic blood flow from 4d mri data. In: 2013 IEEE Pacific Visualization Symposium (PacificVis). 2013, p. 129–136.

[24] Jankowai, J, Englund, R, Ropinski, T, Hotz, I. Interactive 4d mri blood flow exploration and analysis using line predicates. In: Proceedings of SIGRAD 2016, May 23rd and 24th, Visby, Sweden. 127; Linkping University Electronic Press, Linkpings universitet; 2016, p. 35–42.

[25] Meuschke, M, Lawonn, K, Köhler, B, Preim, U, Preim, B. Clustering of aortic vortex flow in cardiac 4d pc-mri data. In: Tolxdorff, T, Deserno, TM, Handels, H, Meinzer, HP, editors. Bildverarbeitung für die Medizin 2016. Berlin, Heidelberg: Springer Berlin Heidelberg. ISBN 978-3-662-49465-3; 2016, p. 182–187.

[26] Oeltze, S, Lehmann, DJ, Kuhn, A, Janiga, G, Theisel, H, Preim, B. Blood flow clustering and applications in virtual stenting of intracranial aneurysms. IEEE Transactions on Visualization and Computer Graphics 2014;.

[27] van Pelt, R, Jacobs, S, ter Haar Romeny, B, Vilanova, A. Visualization of 4d blood-flow fields by spatiotemporal hierarchical clustering. Computer Graphics Forum 2012;31(3):1065–1074.

[28] Gasteiger, R, Neugebauer, M, Beuing, O, Preim, B. The FLOWLENS: A Focus-and-Context Visualization Approach for Exploration of Blood Flow in Cerebral Aneurysms. IEEE Transactions on Visualization and Computer Graphics 2011;17(12):2183–2192.

[29] Djavaherpour, H, Mahdavi-Amiri, A, Samavati, FF. Physical visualization of geospatial datasets. IEEE Computer Graphics and Applications 2017;38(3):61–69.

[30] Taher, F, Hardy, J, Karnik, A, Weichel, C, Jansen, Y, Hornbæk, K, et al. Exploring interactions with physically dynamic bar charts. In: Proceedings of the 33rd Annual ACM Conference on Human Factors in Computing Systems. CHI '15; New York, NY, USA: ACM. ISBN 978-1-4503-3145-6; 2015, p. 3237–3246.

[31] Taher, F, Jansen, Y, Woodruff, J, Hardy, J, Hornbk, K, Alexander, J. Investigating the use of a dynamic physical bar chart for data exploration and presentation. IEEE Transactions on Visualization and Computer Graphics 2017;23(1):451–460.

[32] Houben, S, Golsteijn, C, Gallacher, S, Johnson, R, Bakker, S, Marquardt, N, et al. Physikit: Data engagement through physical ambient visualizations in the home. In: Proceedings of the 2016 CHI Conference on Human Factors in Computing Systems. CHI '16; New York, NY, USA: ACM. ISBN 978-1-4503-3362-7; 2016, p. 1608–1619.

[33] Herman, B, Keefe, DF. Boxcars on Potatoes: Exploring the Design Language for Tangible Visualizations of Scalar Data Fields on 3D Surfaces. In: International Workshop 'Toward a Design Language for Data Physicalization'. 2018,.

[34] Bader, C, Kolb, D, Weaver, JC, Sharma, S, Hosny, A, Costa, J, et al. Making data matter: Voxel printing for the digital fabrication of data across scales and domains. Science Advances 2018;4(5).

[35] Allen, B, Smith, S. Motus Forma: People's Motions in a Shared Space. 2016. URL: `http://dataphys.org/list/motus-forma-peoples-motions-in-a-shared-space/`.

[36] Langnau, L. How to 3d print fluid flow trajectory lines. 2017. URL: `https://www.makepartsfast.com/how-to-3d-print-fluid-flow-trajectory-lines/`.

[37] Taira, K, Sun, Y, Canuto, D. 3d printing of fluid flow structures. 2017. arXiv:arXiv:1701.07560.

[38] Kazi, RH, Grossman, T, Mogk, C, Schmidt, R, Fitzmaurice, G. Chronofab: Fabricating motion. In: Proceedings of the 2016 CHI Conference on Human Factors in Computing Systems. CHI '16; New York, NY, USA: ACM. ISBN 978-1-4503-3362-7; 2016, p. 908–918.

[39] Zhang, X, Dekel, T, Xue, T, Owens, A, He, Q, Wu, J, et al. Mosculp: Interactive visualization of shape and time. In: Proceedings of the 31st Annual ACM Symposium on User Interface Software and Technology. UIST '18; New York, NY, USA: ACM. ISBN 978-1-4503-5948-1; 2018, p. 275–285.

[40] Acevedo, D, Zhang, S, Laidlaw, DH, Bull, C. Color rapid prototyping for diffusion tensor MRI visualization. In: Proceedings of MICCAI 2004 Short Papers. 2004,.

[41] Mitsouras, D, Liacouras, P, Imanzadeh, A, Giannopoulos, AA, Cai, T, Kumamaru, KK, et al. Medical 3D Printing for the Radiologist. Radiographics 2015;35(7):1965–1988.

[42] Byrne, N, Velasco Forte, M, Tandon, A, Valverde, I, Hussain, T. A systematic review of image segmentation methodology, used in the additive manufacture of patient-specific 3d printed models of the cardiovascular system. JRSM Cardiovascular Disease 2016;5:1–9.

[43] Elbaz, MS, van der Geest, RJ, Calkoen, EE, de Roos, A, Lelieveldt, BP, Roest, AA, et al. Assessment of viscous energy loss and the association with three-dimensional vortex ring formation in left ventricular inflow: In vivo evaluation using four-dimensional flow MRI. Magnetic Resonance in Medicine 2017;77(2):794–805.

[44] Elbaz, MS, Calkoen, EE, Westenberg, JJ, Lelieveldt, BP, Roest, AA, van der Geest, RJ. Vortex flow during early and late left ventricular filling in normal subjects: quantitative characterization using retrospectively-gated 4D flow cardiovascular magnetic resonance and three-dimensional vortex core analysis. J Cardiovasc Magn Reson 2014;16:78.

[45] Stratasys Ltd., . The New Face(s) of LAIKA: Voxel print technology enables fully customized facial animation. 2017. URL: `https://www.stratasys.com/resources/search/case-studies/laika`.

[46] Mathews, JH, Fink, KD. Numerical Methods Using MATLAB. 4th ed.; Upper Saddle River, NJ, USA: Prentice-Hall Inc.; 2004. ISBN 0130652482.

[47] Hanson, AJ, Ma, H. Parallel transport approach to curve framing. Tech. Rep.; 1995.

[48] Ayachit, U. The ParaView Guide: A Parallel Visualization Application. USA: Kitware, Inc.; 2015. ISBN 1930934300, 9781930934306.

[49] Desolneux, A, Moisan, L, Morel, JM. From gestalt theory to image analysis: a probabilistic approach; vol. 34. Springer Science & Business Media; 2007.

[50] Cohn, N. The Visual Language of Comics: Introduction to the Structure and Cognition of Sequential Images. A&C Black; 2013.

[51] Pedrizzetti, G, La Canna, G, Alfieri, O, Tonti, G. The vortex - an early predictor of cardiovascular outcome? Nature Reviews Cardiology 2014;11.

[52] Kheradvar, A, Pedrizzetti, G. Vortex Formation in the Cardiovascular System. 2012. ISBN ISBN 978-1-4471-2287-6. doi:`10.1007/978-1-4471-2288-3`.

[53] Sengupta, PP, Narula, J, Chandrashekhar, Y. The dynamic vortex of a beating heart: wring out the old and ring in the new! Journal of the American College of Cardiology 2014;64(16):1722–1724. doi:`10.1016/j.jacc.2014.07.975`.

[54] Jiang, M, Machiraju, R, Thompson, D. Detection and visualization of vortices. In: The Visualization Handbook. Academic Press; 2005, p. 295–309.

[55] Jeong, J, Hussain, F. On the identification of a vortex. Journal of Fluid Mechanics 1995;285:6994. doi:`10.1017/S0022112095000462`.

[56] ElBaz, MSM, Lelieveldt, BPF, Westenberg, JJM, van der Geest, RJ. Automatic extraction of the 3d left ventricular diastolic transmitral vortex ring from 3d whole-heart phase contrast mri using laplace-beltrami signatures. In: Camara, O, Mansi, T, Pop, M, Rhode, K, Sermesant, M, Young, A, editors. Statistical Atlases and Computational Models of the Heart. Imaging and Modelling Challenges. Berlin, Heidelberg: Springer Berlin Heidelberg; 2014, p. 204–211.

Supplementary Material

A supplemental video showcases some of the 3D printed prototypes discussed in the paper.

Conflict of Interest

The authors declare that they have no known competing financial interests or personal relationships that could have appeared to influence the work reported in this paper.

Journal Pre-proof